# Electrical Conductivity of Olivine, a Dunite, and the Mantle

STEVEN CONSTABLE

*Scripps Institution of Oceanography, La Jolla, California*

AL DUBA

*Lawrence Livermore National Laboratory, Livermore, California*

Laboratory studies of the electrical conductivity of rocks and minerals are vital to the interpretation of electromagnetic soundings of the Earth's mantle. To date, the most reliable data have been collected from single crystals. We have extended these studies with electrical conductivity measurements on a dunite from North Carolina, in the temperature range of 600°–1200°C and under controlled oxygen fugacity. Observations of conductivity as a function of oxygen fugacity and temperature demonstrate that conduction in the dunite is indistinguishable from conduction in single olivine crystals. Thus the common practice of exaggerating the single-crystal conductivities to account for conduction by grain boundary phases in the mantle is unnecessary. Because the dunite conductivity is consistent with that published for single crystals under similar conditions, we have made a combined analysis of these data. Conductivity as a function of temperature between 600° and 1450°C displays three conduction mechanisms whose activation energies may be recovered by nonlinear least squares fitting, yielding activation energies of $0.21 \pm 2.56 \times 10^{-19}$ J ($0.13 \pm 1.60$ eV) below 720°C, $2.56 \pm 0.02 \times 10^{-19}$ J ($1.60 \pm 0.01$ eV) between 720°C and 1500°C and $11.46 \pm 0.90 \times 10^{-19}$ J ($7.16 \pm 0.56$ eV) above 1500°C. The behavior of conductivity as a function of oxygen fugacity is well explained by a model in which an $f_{O_2}$-independent population of charge carriers is supplemented at high oxygen fugacities with a population that is proportional to $f_{O_2}{}^{0.3}$. This parametrization produces a clear correlation of the $f_{O_2}$ dependent term with iron content, which is otherwise obscured by variations in conductivity among olivines.

## INTRODUCTION

Estimates of the electrical conductivity of Earth form an important part of our understanding of our planet's interior. Observations of the response of Earth to an applied electromagnetic field, either of natural or man-made origin, give us a direct measurement of bulk mantle conductivity, in situ, although the deconvolution of the electromagnetic response to obtain conductivity is by no means a trivial operation. While we might use Earth conductivity estimates to infer structure, as delineated by domains of differing conductivity, the use of laboratory measurements of conductivity for rocks and minerals allows us to go further and to estimate temperature, phase state, fluid content, and even mineralogy. To do this, we must replicate as many of the in situ conditions of the mantle as possible. The focus of this paper is a laboratory study of the conductivity of a rock composed primarily of olivine, under conditions which might represent those of the upper mantle to the depth of the 400-km seismic discontinuity.

*Importance of Laboratory Conductivity Measurements*

Perhaps the most important use of laboratory conductivity data is the estimation of temperature within Earth. In the absence of volatiles or conductive grain boundary phases, the electrical conductivity of a silicate rock is strongly dependent on temperature. If one can infer mantle mineralogy using information such as density, seismic velocity, and composition of volcanic nodules, then laboratory conductivity–temperature measurements may be combined with observational conductivity–depth estimates [obtained from geomagnetic and electrical sounding] to give a temperature–depth relationship; an electrogeotherm [*Duba*, 1976].

A second, less well developed, use of the laboratory measurements is to constrain the interpretation of observational conductivity–depth data. If laboratory data can provide lower and upper limits on the conductivity of mantle material as a function of temperature and if one has an idea, a priori, of the geotherm, then mantle conductivity may be predicted. One approach might then be to ask whether the observational data are consistent with this prediction. Agreement reinforces the assumptions made; disagreement directs attention to the need for more work. Note that this approach does not necessarily require the generation of a model to fit the observational data, and so the problem of nonuniqueness in the interpretation of geomagnetic data does not arise. Another approach is to combine the laboratory predictions with the observational data to improve one's model of Earth conductivity. For example, the controlled source experiment of *Cox et al.* [1986] was sensitive to mantle structure deeper than about 15 km, but this deep structure was highly correlated with shallower structure. By constraining the deep structure to follow upper and lower bounds of conductivity inferred from the laboratory studies, the shallow structure was better resolved. However, the upper bound used by Cox et al. was derived from a rather ad hoc extrapolation of single crystal olivine conductivity. Furthermore, there were no olivine conductivity data applicable to the cooler temperature regime associated with the uppermost oceanic mantle.

### Olivine as a Mantle Analogue

The upper mantle is thought to be composed primarily of the minerals olivine and pyroxene, olivine being the dominant mineral both in terms of its volume fraction and its electrical conductivity [*Duba, Boland and Ringwood*, 1973]. This dominance has led to the extrapolation of the properties of the mineral olivine to the properties of the rock peridotite, which is a constituent of the upper mantle. From the point of view of many laboratory studies, including those used to measure conductivity, there is great advantage in using single crystals of minerals over using whole rocks. The sample size can be small and still representative of the larger material, the problems of maintaining grain to grain cohesion at temperature are avoided, the possible phases and phase transitions are greatly simplified (a given temperature path in a multiphase system will usually cross several phase boundaries), the grain boundary phases due to weathering near Earth's surface can be avoided, and the physical interpretation of the data is less ambiguous. The complexities of studying whole rocks may be better appreciated if one recalls that the conduction mechanism in olivine is still a matter of study [*Schock, Duba and Shankland*, 1989]. On the other hand, Earth is made of rock, and extrapolation from single crystal data to the mantle environment must be made at some point. We address one aspect of this extrapolation in this paper, taking the step from a single mineral crystal to a nearly monomineralic, polycrystalline rock.

Good single-crystal conductivity data for olivine are already available, at least at relatively high temperatures. One data set that we consider reliable and which will be used later in this paper is that of *Duba, Heard and Schock* [1974]. These data are for a single crystal of Red Sea peridot (RSP) in the [010] crystallographic direction, measured between about 900° and 1600°C. Pressure was varied but shown to have little effect, less than that of a 5 C° change in temperature. More importantly, oxygen fugacity ($f_{O_2}$), equivalent to partial pressure for an ideal gas at the conditions of the experiment, was controlled. The log of the electrical conductivity of olivine has been observed to vary as $f_{O_2}^{1/7}$ at the temperatures under discussion [*Schock and Duba*, 1985], that is, the more oxidizing the atmosphere, the more conductive the olivine. Furthermore, leaving the stability field of olivine because of inadequate fugacity control will irreversibly produce iron or magnetite, both of which have a marked effect on conductivity [*Duba and Nicholls*, 1973].
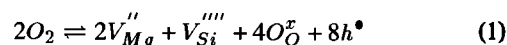
A geophysical mythology arose around attempts to extrapolate these single-crystal data to mantle conditions. One of the big questions was the role of grain boundaries on conduction. It seemed reasonable to suppose that grain boundary phases would increase the bulk conductivity of an olivine-rich rock over that measured for a single olivine crystal. *Shankland and Waff* [1977] multiplied the RSP data of *Duba et al.* [1974] by a factor of 10 to obtain an upper bound on mantle conductivity. The context within which this was done was a study of the effect of partial melt on conductivity; the authors wanted to see what effect increasing the matrix conductivity would have on a rock whose conduction was dominated by interstitial melt. However, the RSP×10 idea was reinforced by *Shankland* [1981, p. 258], who again presented it as a model for polycrystalline olivine, stating that "conductivities about 1-1/2 orders of magnitude above Red Sea peridot are at least plausible". This idea spread, and, for example, *Jones*

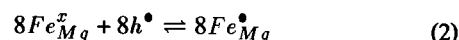[1982] and *Cox et al.* [1986] both used RSP×10 as limits on mantle conductivity.

### Electrical Conduction in Olivine

Many years of research and speculation have failed to provide a definitive explanation for the electrical conduction mechanism in olivine at geophysically interesting temperatures, although recent data [*Schock et al.*, 1989] have made the educated guesswork more reliable. One critical observation is that forsterite [$Mg_2SiO_4$, or $Fo_{100}$] has a different conduction mechanism than naturally occurring olivine [approximately $Mg_{1.8}Fe_{0.2}SiO_4$, or $Fo_{90}$], based on differing magnitudes of conductivity, thermoelectric effects, dependence on $f_{O_2}$ and dependence on crystallographic direction. This suggests that the iron in natural olivine is involved in the conduction process. The positive $f_{O_2}$ dependence of olivine conductivity requires that incorporation of oxygen gas into the crystal lattice generates an appropriately larger population of charge carriers. The curvature in the conductivity–temperature data at 1200°-1500°C [*Duba et al.*, 1974; *Schock et al.*, 1989] indicates that there is a change in conduction mechanism around these temperatures. This is supported by the observation of *Schock et al.* [1989] of an associated change in sign in the thermoelectric coefficient, from positive to negative, at 1390°C and hence a change from positive charge carriers to negative carriers at this temperature.

The mechanism presented by Schock et al. for conduction below 1390° is the generation of electron holes in the valence band and cation vacancies by incorporation of oxygen into the lattice:

$$2O_2 \rightleftharpoons 2V''_{Mg} + V''''_{Si} + 4O^x_O + 8h^\bullet \tag{1}$$

These holes are then accepted by the iron substituting at the magnesium sites:

$$8Fe^x_{Mg} + 8h^\bullet \rightleftharpoons 8Fe^\bullet_{Mg} \tag{2}$$

Thus the holes are not free to move in the valence band but are trapped by the iron. For sufficient iron concentrations the holes can "hop" from one iron ion to another, with a mobility more characteristic of ionic conduction than band conduction, a hopping mechanism first suggested by *Bradley et al.* [1964]. This model predicts that electrical conductivity will increase with iron content, and although this holds in the step from forsterite to olivine, within olivines there are exceptions to this correlation [*Duba*, 1972].

Above 1390°, where the sign of the carrier changes to negative, *Shock et al.* [1989] favor ionic conduction by the magnesium vacancies, $V''_{Mg}$, generated by the oxygen. They observed that since ionic and electronic conduction have opposite pressure coefficients, this model accounts for the small pressure effect observed for olivine by *Duba et al.* [1974] and *Shock et al.* [1977].

### This Study

A polycrystalline rock composed primarily of olivine represents the next complication over the single crystal measurements. Dunites are a naturally occurring approximation to monomineralic olivine rock. Minor pyroxene and oxides are likely to exist but in quantities small enough for one to expect that the dominant conduction will be through the olivine. Weathering is a concern; most dunites will have appreciable

serpentine and talc on the grain boundaries. However, such a rock has the advantage of being a natural assemblage of minerals and grain boundaries and, if not significantly altered, can provide information on the electrical behavior of real rocks without the complications associated with synthetic materials made by crushing and sintering olivine [Shock et al., 1977]. Even very carefully prepared polycrystalline compacts [Karato et al., 1986] can have features such as bubbles inside grains which are not common in natural samples.

The sample used in this study is a dunite from Jackson County, North Carolina, probably part of the Balsam Gap body [Astwood et al., 1972; see also Lipin, 1984]. The olivine is granular with a grain size of 0.1-1.0 mm. Based on work by Lipin [1984] and Astwood et al. [1972], thin section examination, and electron microprobe analysis, the olivine averages $Fo_{92.7}$ with no preferred crystallographic orientation. The sample is remarkably unaltered, with no serpentine visible in thin section and little grain boundary phase evident in microprobe examination (Figure 1). No pyroxene is evident, the only minor mineral being chromite in quantities of less than 1%. Even smaller quantities of chlorite are found in association with the chromite. The

specimens used were disks, typically 0.75-1 mm thick and 7.5 mm diameter.

The apparatus used for conductivity measurement as well as oxygen fugacity control and measurement is described in Duba et al. [1990]. It is basically a vertical, cylindrical alumina assembly whose central portion is heated by a furnace. Two thermocouples, each entering from opposite ends of the cylinder, serve as both temperature measurement and as electrodes to measure the transverse resistance, as the sample discs are inserted between the platinum thermocouple foils of the apparatus. One departure from standard procedures was in the matter of electrodes which provide contact between the sample and the thermocouple foil to which the platinum and platinum 10% rhodium wires are welded. For experiments that were not to exceed 1000°C, 0.025-mm gold foils were placed between the sample and the thermocouple foils; experiments above 1000°C had 0.025-mm platinum foils. It is known that at high temperature and low oxygen fugacity, olivine can lose iron to platinum and suffer a loss of conductivity, but we have been careful to avoid such conditions by limiting the temperature to 1200°C. The reproducibility of conductivity on heating and cooling provides a check that no significant
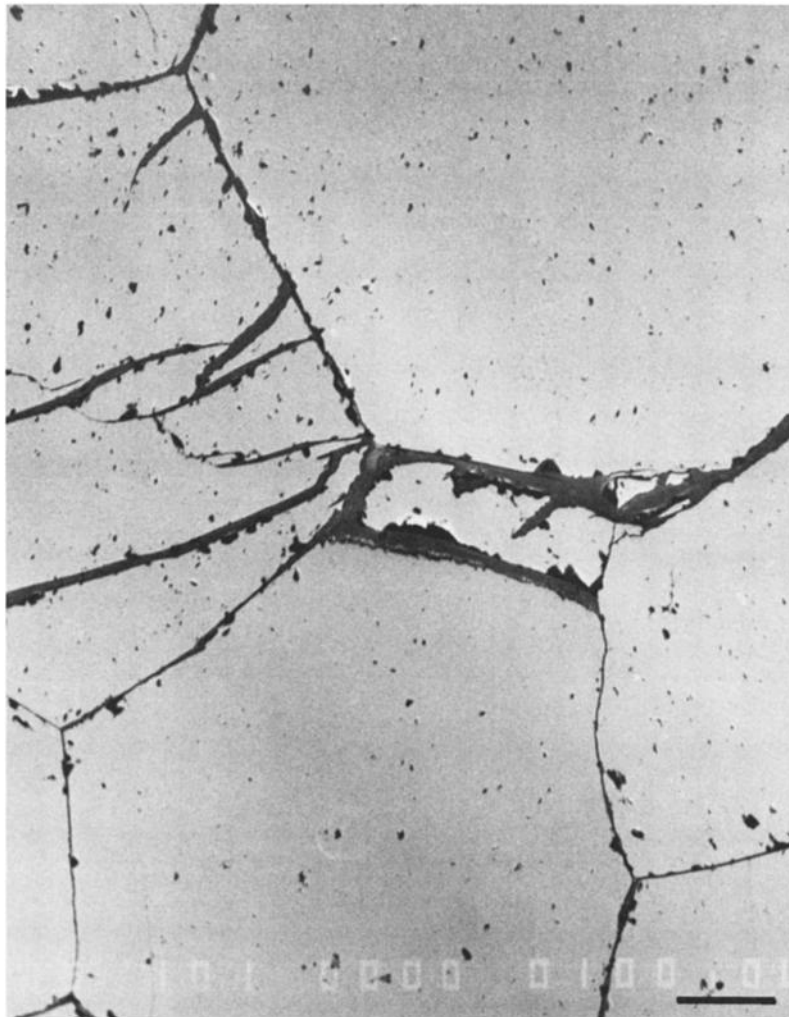


Fig.1. Electron probe photomicrograph showing olivine grain boundaries. Although generally clean, the grain boundaries exhibit very small amounts of a low atomic number phase. This phase is a hydrous, aluminum–magnesium silicate containing about 2% each FeO and $Cr_2O_3$. Although generally described as serpentine, the high Cr implies that it is not a weathering product of olivine. The horizontal bar is 100 $\mu$m long.

iron loss has occurred. The accuracy of this apparatus is about 2 C° in temperature and 1% in conductivity.

Oxygen fugacity is controlled by continuously passing a metered mix of $CO_2$:CO through the apparatus at atmospheric pressure. Fugacity is measured using a calcia-doped zirconia sensor situated in another furnace assembly but in series with the gas mix used in the conductivity experiment.

The rate of temperature change during conductivity measurement was 1 C°/min. It was originally at 1/3 C°/min in order to minimize thermal shock to the polycrystalline sample. However, this practice was discontinued as this slow heating rate allowed the production of considerable carbon at low temperature because of the long time spent in the carbon field of a particular gas mixture [Deines et al., 1974], and allowed oxidation in the temperature range where the gas mixture was out of oxygen fugacity equilibrium (below about 500°C). Since no effect of thermal cracking on conductivity was observed, in order to minimize these effects the heating and cooling rates were increased to 2 C°/min below 600°C.

## RESULTS

### Oxygen Fugacity Control

We have stated that it is necessary to control oxygen fugacity during the experiment, both to ensure reproducible conductivities and to maintain the olivine within its stability field. Figure 2 shows the stability field of olivine in temperature–oxygen fugacity space, the stability fields of iron and iron oxides (which may be present in the rock either naturally or as a result of metamorphism of the olivine during the experiment), the equilibrium for the carbon oxidation reaction, and finally the theoretical equilibrium curves for mixtures of $CO_2$:CO of 1:1 and 30:1.

The use of gas mixes to control oxygen fugacity works well at temperatures high enough for the gases to be in equilibrium, or above about 700°C. Figure 3 shows the experimentally determined oxygen fugacity for a gas mix of 1:1 $CO_2$:CO between 400° and 1160°C, with the theoretical 1:1 curve shown for comparison. As can be seen, the experimentally measured fugacities are close enough to the theoretical values to obscure the curve above 800°. At low temperatures, however, we run into three problems:

1. The gases constituting the mix are not in equilibrium, so the oxygen fugacity obtained is not that suggested by the assumption of equilibrium. Any oxygen contaminating the gases is not consumed by the reaction fast enough to prevent the mix being too oxidizing for olivine.

2. The zirconia cell used to measure the experimental oxygen fugacity is itself not in equilibrium at these low temperatures, probably failing to measure oxygen fugacity correctly below about 500°C.

3. When the oxygen fugacity falls to that of the equilibrium in the reaction $CO_2 = C + O_2$, the gas mix will precipitate carbon [Deines et al., 1974]. The phase boundary for this reaction is drawn in Figures 2 and 3.

We have observed oxidation of the olivine to haematitite at low temperatures, presumably because of problem 1, contaminant oxygen not being consumed. This is not a reversible reaction, as once iron leaves olivine it is stable in the oxide phases throughout our experimental regime. We have attempted to avoid oxidation by conducting the initial heating in a relatively reducing atmosphere (1:1 gas mix) and doubling the normal heating rate to 2 C°/min while heating up to 600°C. Similarly, the cooling rate is doubled below 600°C. The use of a more reducing atmosphere



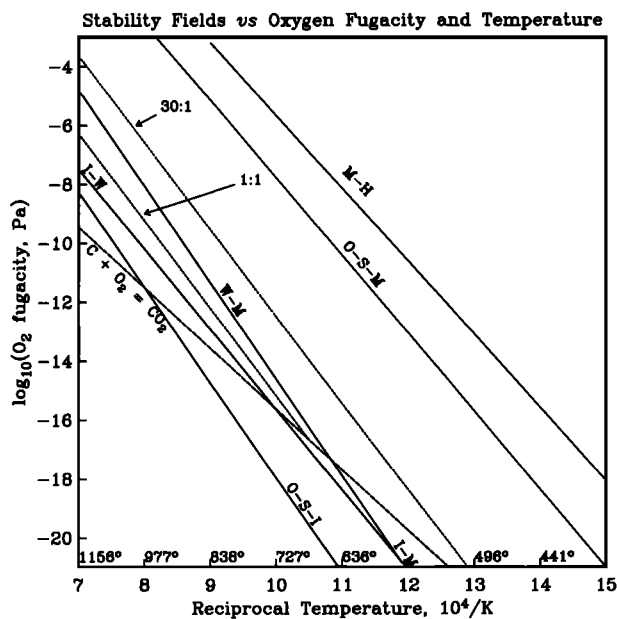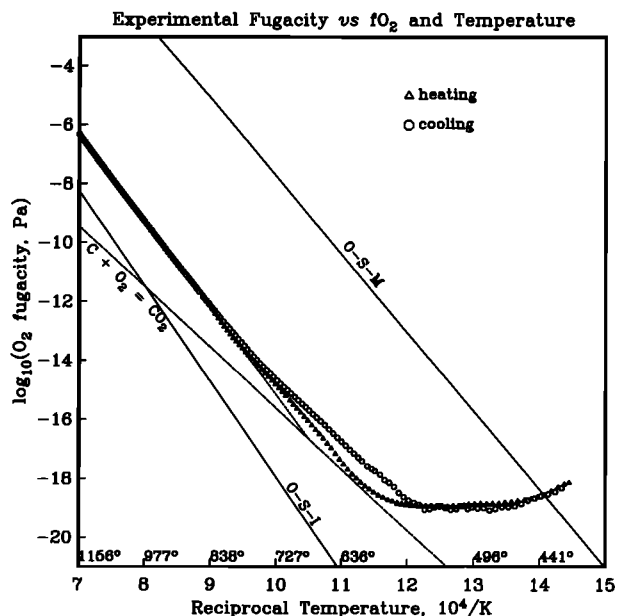**Stability Fields vs Oxygen Fugacity and Temperature**

Fig. 2. The stability fields of olivine and iron oxides shown as a function of $f_{O_2}$ and $1/T$. M, magnetite; H, haematite; O, olivine; S, silica; W, wüstite; I, iron [Huebner, 1971]. Also shown are the theoretical $f_{O_2}$:$1/T$ relationships for gas mixes of 30:1 and 1:1 $CO_2$:CO [Deines et al, 1974]. The $CO_2 = C + O_2$ equilibrium shows where carbon will drop out of the gas mix and represents the lower limit on fugacity control with these gases.



**Experimental Fugacity vs fO₂ and Temperature**

Fig. 3. Experimental $f_{O_2}$ data for a mix of 1:1 $CO_2$:CO [triangles, heating; circles, cooling] follows [and obscures] the theoretical 1:1 curve above 800°C. The experimental data follow a path which is too oxidizing below 550°C because here it is too cool for the gas mix to reach equilibrium in the experimental time frame, and so oxygen contaminating the gases is allowed to persist. The experimental path is slightly more oxidising on cooling for similar reasons: reequilibrium is not complete and a memory of the higher-temperature, more oxidizing condition, persists.

exacerbates the precipitation of carbon but, since oxidation is an irreversible reaction, this is considered the lesser evil since the precipitated carbon is consumed above about 700°C in the $CO_2/CO$ mixtures used here.

The precipitation of carbon is often evident at low temperatures for all the gas mixes used in our experiment. The occurrence of carbon is not easily predictable, as it depends on gas mix, heating rate, and previous history of the furnace assembly. Generally speaking, in a carbon free furnace assembly, carbon will not precipitate and affect conductivity measurements at gas mixes of 3 $CO_2$:$CO$ and higher at heating rates of 1 C°/min. No matter what the previous history of the furnace assembly, a mix of 1:1 or less will precipitate carbon sufficient to affect conductivity measured at at heating rate of 1 C°/min.

Carbon is, of course, a very good conductor and makes the determination of olivine conductivity impossible. Since we see the effect of carbon precipitation in the conductivity data as low as 350°C, the experimental oxygen fugacity path must follow the $CO_2 \rightleftharpoons C + O_2$ equilibrium boundary up to the point where the gas mix oxygen fugacity meets the carbon precipitation curve, or around 670°C for a 1:1 mix. The oxygen fugacity can never go below the $CO_2 \rightleftharpoons C + O_2$ equilibrium boundary because the oxygen generated as carbon precipitates has a negative feedback effect.

Carbon precipitation is a reversible reaction because it will be burnt off when the sample reaches higher temperatures. We see a dramatic reduction in conductivity for a 1:1 gas mix as the heating cycle goes through 670°and the oxygen fugacity equilibrium leaves the carbon precipitation region (Figure 4). It takes a little more time and temperature to remove all the carbon, because carbon has been deposited in the cooler parts of the apparatus and may migrate onto the sample during subsequent cooling/heating, but as long as we avoid cooling the sample below 670° at a gas mixture of 1:1, we can make measurements on a sample free of carbon after initial heating.
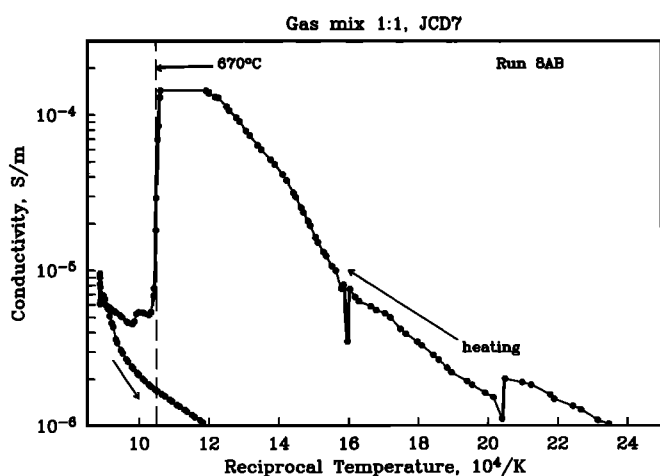
From Figure 2 we see that for a fixed gas mix, $f_{O_2}$

**Gas mix 1:1, JCD7**



Fig. 4. A heating and cooling run at a gas mix of 1:1 $CO_2$:$CO$ in which carbon has precipitated on the sample below 670°C. The jagged conductivity curve is typical of carbon as contact between films of the contaminant are made and broken. At 670° [for this gas mix] the carbon stability field is left and the carbon is burned [oxidized] off, accompanied by a dramatic drop in conductivity. Residual carbon is removed after spending time above 670°, and the cooling curve follows the path for olivine conduction.

changes as a function of temperature. Since the slope of this change is very nearly parallel to the olivine stability field, as well as being subparallel to the quartz-fayalite-magnetite and wüstite-iron models of mantle $f_{O_2}$ [e.g. *Ulmer et al.*, 1987], a fixed gas mix is convenient for these experiments. However, there are two errors associated with use of fixed gas mixes: Activation energies produced from conductivity–temperature measurements will include a component due to the conductivity dependence of the sample on oxygen fugacity [*Schock et al.*, 1989], and the samples do not achieve equilibrium with the gas during the changes in $f_{O_2}$ associated with heating and cooling. Both these errors result from the oxygen fugacity dependence of conductivity and may be quantified.

Based on observations of the small changes in conductivity associated with different fugacities, the specimens re-equilibrate after changes in oxygen fugacity on a time scale of a few tens of minutes. Equilibration of the sample at 1200°C after the gas mix was changed from 1:10 to 10:1 $CO_2$:$CO$, corresponding to an $f_{O_2}$ change of $10^{-8}$ Pa to $10^{-4.3}$ Pa, exhibited a characteristic time of about 25 min. This delay in the response to a change in $f_{O_2}$ produces a discrepancy between heating and cooling cycles, with the cooling cycle always being more conductive than the heating cycle because the higher $f_{O_2}$/higher conductivity state from the higher temperatures is not immediately lost as the temperature is lowered. Similarly, on heating, the higher conductivity/higher $f_{O_2}$ state is not immediately achieved and so the measurements are always a little too resistive. We can use the measured equilibration times to predict the hysteresis that will result from using a given heating or cooling rate. The exponential response to a step in oxygen fugacity can be differentiated to obtain the impulse response of the system. If the impulse response is convolved with a ramp switched on at time zero [corresponding to cooling the sample after being held at the highest temperature for several hours], then the response of the system to a given heating/cooling rate can be obtained. The response of the system at time $t$ to being cooled (or heated, if the sign is changed appropriately) at $\theta$ degrees per minute is

$$\sigma(t) = \sigma(T) - \theta A t + \theta A \tau(1 - e^{-t/\tau}) \qquad (3)$$

where $\tau$ is the characteristic time of the equilibration to a new $f_{O_2}$ and $T$ is the temperature. $A$ is a term describing the conductivity dependence on temperature which results from $f_{O_2}$ variation. $A$ is obtained by taking the magnitude of the conductivity dependence on oxygen fugacity multiplied by the oxygen fugacity dependence on temperature for the fixed gas mix. That is,

$$A = \frac{\partial \sigma}{\partial T_{fO_2}} = \frac{\partial \sigma}{\partial fO_2} \frac{\partial fO_2}{\partial T}$$

$A$ and $\tau$ both depend on temperature and so this expression is valid only at a given temperature, or an approximation for a small temperature range.

The first term, $\sigma(T)$, is the conductivity dependence on temperature that we wish to measure. Since $\theta t$ is the total change in temperature accomplished by heating or cooling, the second term in expression (3) is the change in conductivity due to changes in oxygen fugacity. The third term in the expression is the error which results from lack of equilibration during heating and cooling. A conductivity–temperature plot will have a heating/cooling discrepancy of twice this value

since there is a contribution from heating as well as cooling. At $t = 0$ there is no error and at $t \gg \tau$ the error obtains the maximum value of $\theta A\tau$.

The above analysis predicts the hysteresis between heating and cooling very well for experiments on San Carlos olivine above 1200°C. However, very little hysteresis is seen in the dunite conductivity–temperature plots below 1200° (Figure 8). One might consider using this analysis to correct data such as those from San Carlos olivine for the effects of $f_{O_2}$ in order to recover the $\sigma(T)$ term, whose activation energy is that of the physical conduction process. This correction, however, requires extrapolation in temperature, as all data on $A$ have been gathered at 1200°C only, and we are reluctant to perform the correction exercise until we have data for $A$ at other temperatures. Furthermore, one objective is to measure conductivity under mantle conditions and, as we have shown (Figure 2), $\partial f O_2 / \partial T$ follows models of mantle fugacity for the gas mixes used in these studies. Interpreted activation energies thus incorporate predictions for changes of $f_{O_2}$ in the mantle with temperature.

## Conductivity Versus Oxygen Fugacity

The dependence of conductivity on oxygen fugacity for our dunite sample is shown in Figure 5 (circles). The measurements were all made close to 1200°C and corrected to exactly 1200° using the known dependence of conductivity on temperature discussed below. Several observations can be made: The dunite's behaviour is very similar to that of the two single crystals studied by Schock et al. [1989], represented in Figure 5 by the [010] directions of RSP (triangles) and San Carlos olivine (diamonds). For all the olivines, including the dunite, the oxygen fugacity dependence diminishes below about $10^{-5}$ Pa. We observe also that the 1/7 dependence of conductivity on oxygen fugacity which is much quoted in the literature is merely a simplification. It clearly only applies at the more oxygen rich atmospheres in which olivine is stable (the stability field at 1200° is from about $10^{-8.5}$ Pa to about $10^{-0.5}$ Pa). Furthermore, much of the data collected defines a smaller slope. The dunite has about a 1/8 dependence above $10^{-5}$ Pa and San Carlos olivine has about a 1/11 dependence for the [100] and [010] directions (the [001] direction is slightly steeper at about 1/8 [Schock et al., 1989]).

The independence of conductivity on oxygen fugacity below about $10^{-5}$ Pa suggests a new model for conductivity as a function of oxygen fugacity, in which an $f_{O_2}$ independent population of charge carriers exists at low $f_{O_2}$, supplemented at higher $f_{O_2}$ by additional charge carriers generated by the absorption of oxygen. The base population obscures the $f_{O_2}$ dependent behaviour until the $f_{O_2}$ is high enough for the second population to dominate. Our new model is

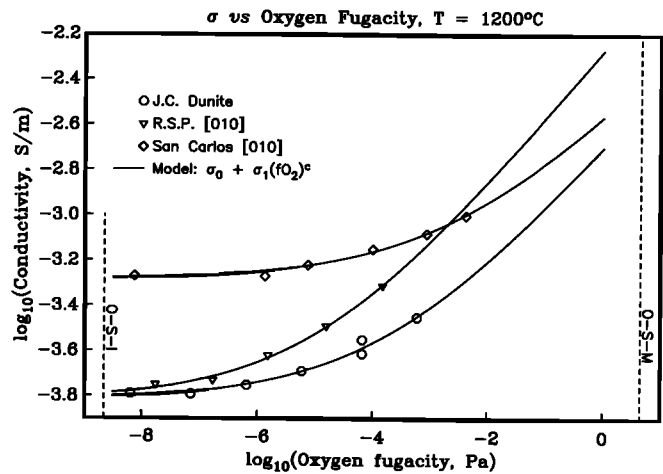$$\sigma = \sigma_0 + \sigma_1 (f O_2)^c \qquad (4)$$



Fig. 5. Conductivity versus oxygen fugacity for Jackson County dunite [circles]. The data were collected within a few degrees of 1200°C and corrected to 1200° using the known temperature dependence of conductivity. For comparison, similar data collected on Red Sea peridot [triangles] and San Carlos olivine [diamonds] by Shock et al. [1989] are also shown. The solid lines are fits to the individual data sets of the model $\sigma = \sigma_0 + \sigma_1 [fO_2]^c$.

The second term is the traditional notion of oxygen fugacity dependence, where $c$ has been experimentally determined to be about 1/7 but from equation (1) should be 1/5.5. The $\sigma_0$ term is the base conductivity added to the expression to account for the zero slope of the data at low $f_{O_2}$.

Allowing $\sigma_0$, $\sigma_1$, and $c$ all to be free variables allows us to use least squares to fit the three data sets in Figure 5 separately, to within about 3%. The fits are given in Table 1, and the responses of the models are shown by the lines in Figure 5. The first observation is that the $f_{O_2}$ dependence, characterized by the exponent $c$, is the same (within statistical uncertainty) for all three samples, as one would expect from the physical interpretation of the model. Note that previous interpretations would have fitted the average slope of the data for each sample and so considered the oxygen fugacity dependence different for each sample. The weighted average of the three exponents is $c = 0.296 \pm 0.028$, implying a dependence of 1/3.1 to 1/3.7, higher than anticipated. However, we have to be careful when combining the dunite data with the single crystal data for the [010] direction, as the dunite conductivity samples a random mix of all three crystallographic directions. (We choose the [010] direction for comparison because this is the only direction for which data exist below 1200°C.)

We may now observe that the higher iron content RSP has a higher $\sigma_1$ than the lower iron San Carlos olivine, in spite of having lower conductivities in the oxygen fugacity

TABLE 1. Parametric Fits to Conductivity–Fugacity Data

| Data Set | $\sigma_0$ (S/m) | $\sigma_1 (S/m)$ | $c$ | % RMS |
|---|---|---|---|---|
| Red Sea olivine | -3.81±0.03 | -2.28±0.02 | 0.310±0.04 | 2.6 |
| San Carlos olivine | -3.29±0.02 | -2.65±0.12 | 0.274±0.05 | 2.7 |
| J.C. dunite | -3.82±0.03 | -2.73±0.20 | 0.296±0.06 | 4.1 |

The table presents fits of equation (4) to the data sets in Figure 5. Errors are one standard deviations based on the assumptions of linearity and lack of covariance, both of which are known to be only approximations to the truth. % RMS is the root mean square of the data residuals, expressed as a percentage of the linear conductivities.

range of the measurements. Thus there is now a clear correlation between iron content and conductivity (Figure 6). The dunite data are consistent with this model, but again one must bear in mind that the dunite is a mix of all crystallographic directions, while the single crystal data are only in the [010] direction. One can make a correction for this based on the work of T.J. Shankland and A. Duba (Standard electrical conductivity of isotropic, homogeneous olivine in the temperature range $1100°$-$1500°C$, submitted to *Journal of Geophysical Research*, 1989). This correction predicts that at $1200°C$ the [010] direction for olivine will be about 0.15 orders of magnitude more resistive than the average. Making this correction produces colinear data with a slope of 0.24 orders of magnitude per mole percent iron. We can make the prediction that $Fo_{100}$ in the [010] direction will have a conductivity of $10^{-4\ 6}$ S/m at $1200°C$ if there is no contribution from $\sigma_0$. Schock et al. [1989] measured it to be about $10^{-5\ 0}$ S/m.

Our very simple model, which is a classic expression of mixed extrinsic and intrinsic conduction, provides a self-consistent explanation of the variations observed in the oxygen fugacity dependence of olivine conductivity. We make the prediction that at high $f_{O_2}$ the conductivity will be a clear function of iron content and have an equal slope for all samples. The reader must bear in mind that we are presenting a parametric model only. While the physical interpretation of the $\sigma_1$ term is straightforward, the $\sigma_0$ term is less easily described. Schock et al. [1989] interpreted the lower slope at low $f_{O_2}$ to be caused by production of defects associated with exsolution of nickel–iron. However, the dunite conductivity is reproducible after being at low $f_{O_2}$, both in terms of temperature cycling and cycling within $f_{O_2}$

at fixed temperature. Nor do we see significant changes in conductivity as a function of time [after initial equilibration to the new $f_{O_2}$ state] even after the dunite was held at these lower $f_{O_2}$ conditions for 43 hours. This all suggests that there is no irreversible metamorphism taking place, even though we are quite close to the edge of the stability field. We cannot be exsolving nickel–iron.

At $1200°C$, conduction is purely by means of one mechanism, regardless of $f_{O_2}$. This is evident in the linear nature of the conductivity-$1/T$ plots shown later, and may be quantified for the San Carlos data to show that at $1200°C$ conduction is 99.98% by means of a single mechanism. The charge carrier which is generated by increasing $f_{O_2}$ will have some thermally activated base population, which would explain the presence of a constant $\sigma_0$ term. However, it is difficult to see how a thermally activated term could vary half an order of magnitude between olivines. The cause of this variation in the $\sigma_0$ term is a matter of speculation at this time. There are no patterns in major or trace element chemistry which explain the observed pattern of conduction nor in dislocation density. We do, however, observe a correlation between $\sigma_0$ and the genesis of the olivines. The San Carlos specimen, with the highest $\sigma_0$, is thought to be mantle olivine. The other two olivines, R.S.P. and J.C. dunite, have been metamorphically regrown and have similar, smaller $\sigma_0$. We speculate that the San Carlos olivine has been oxidised in some way, freezing in a population of defects which is higher than in the olivines of crustal origin.

## Conductivity Data

Figure 7 shows conductivity data on an early experiment (on sample 4, or JCD4) where we avoided heating above $700°C$ for fear of thermally cracking the specimen. The oxygen fugacity was controlled with a gas mix of 50:1 and the heating and cooling rate was 0.5 $C°$/min. Enhanced conduction during the dehydration of serpentine and talc is
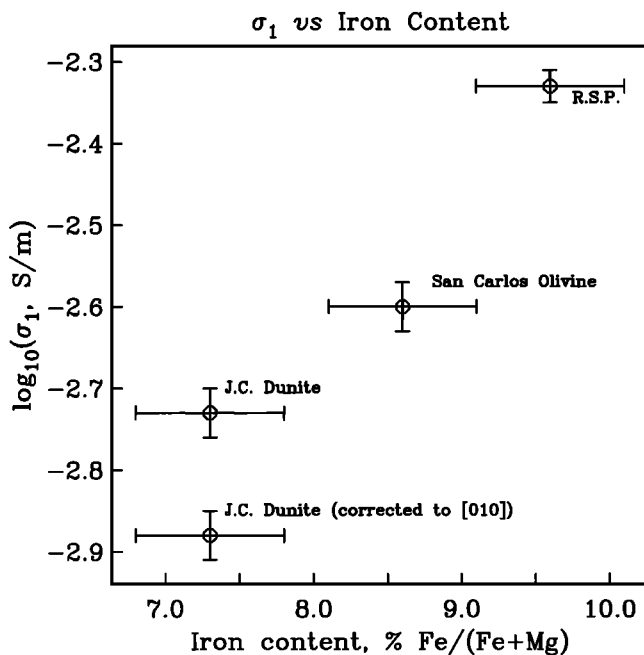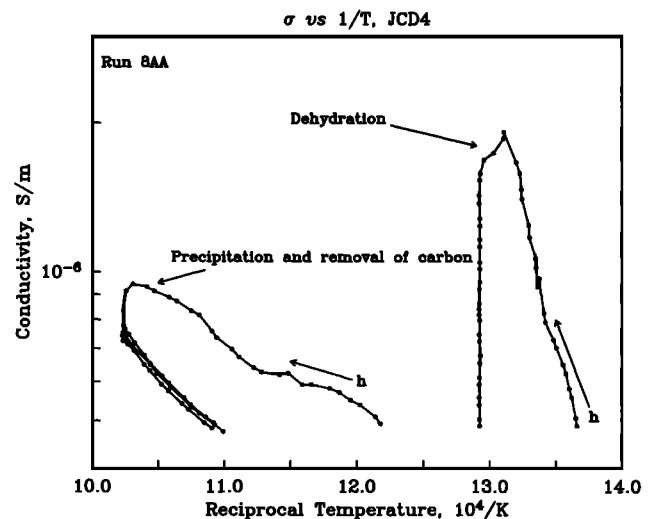


**$\sigma_1$ vs Iron Content**

Fig. 6. The multiplier of the oxygen fugacity dependent term in the proposed model versus iron content for the three olivines under examination. A clear correlation is evident, which is not visible in the raw conductivity data. The correction for the dunite is based on the computations of T.S. Shankland and A. Duba [submitted manuscript, 1990] which indicate that randomly oriented olivine grains will have a conductivity at $1200°C$ that is about 0.15 orders of magnitude larger than the conductivity in the [010] direction.



**$\sigma$ vs 1/T, JCD4**

Fig. 7. Dunite conductivity versus temperature for one complete run at 50:1 $CO_2$:$CO$ mix. On initial heating to $500°C$ dehydration of the sample is accompanied by increased conductivity. During this time, adsorbed water is driven off, and any serpentine in the sample decomposes, producing water. Carbon is then produced from the gas mix, again enhancing conductivity, but is burned off as the sample is held at $700°C$. The sample may then be cycled between $500°$ and $700°$, following a reproducible conductivity path.

apparent, disappearing at 500°. We then see the effect of carbon, which is burned off by holding the specimen at 700° for several hours. Once the carbon was removed, we were able to generate reproducible data during three heating/cooling cycles.

During subsequent runs we heated the specimen to 1200°C, as cracking did not appear to be a problem. The data are highly reproducible, and at the end of the experiments most samples remained intact. Figure 8 presents data from a representative run in which sample 7 (JCD7) was heated to 1200° in an atmosphere of 10:1 $CO_2$:CO. Heating and cooling are indicated and were done at a rate of 1 C°/min. Initial heating to 600°C was carried out at 2 C°/min in an atmosphere of 1:1 as described above. It is clear that we have obtained the reproducibility necessary to demonstrate that no irreversible metamorphism is taking place. The hysteresis at low temperature (below 800°) is probably due to the sample not reaching equilibrium after cooling from high temperatures; the larger defect population associated with the higher oxygen fugacity and high temperature has not yet been lost. Sample JCD4 (Figure 6) shows much less evidence of hysteresis, probably because of the lower heating/cooling rate and lower slope of $\sigma(T)$. Although the greater thickness of JCD7 prevented measurement of conductivity below 700°, the agreement with the data presented in Figure 6 for JCD4, collected below 700°, is good. This suggests that the hysteresis in JCD7 does not totally distort the conductivity behavior. However, throughout this work, quantitative interpretation is restricted to heating data only, which are not distorted by high temperature changes which persist on cooling.

We observe no significant dependence of conductivity on frequency (Figure 9), indicating absence of grain boundary or electrode effects. The dispersion that we see at 10 kHz is due to slight crosstalk between electrode leads; larger at lower temperature where impedance is higher. Figure 9 gives us confidence in the extrapolation of the laboratory
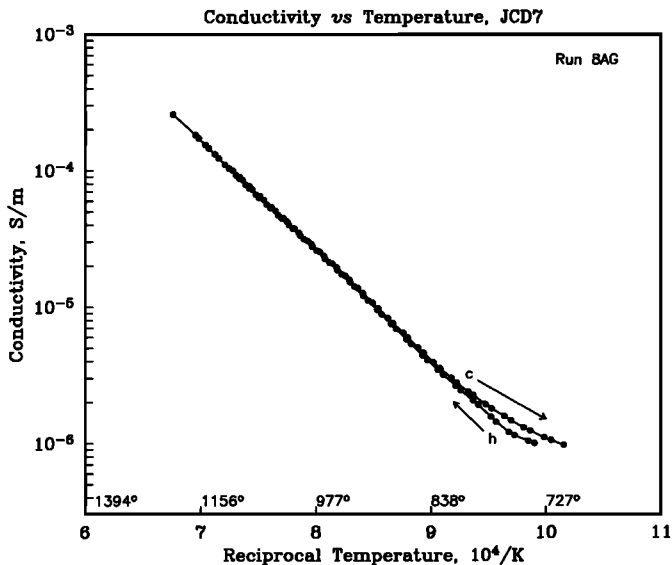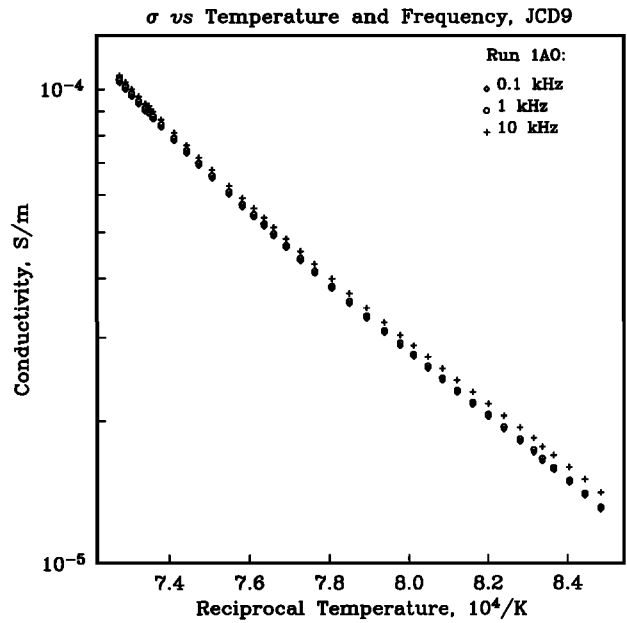


Fig. 9. An example run for the dunite at a gas mix of 10:1. The sample is subjected to increasing temperature and conductivity measured at three different frequencies. The data are highly reproducible and show little evidence of frequency dispersion.

measurements to the frequencies used in geomagnetic and electrical soundings, which extend from 25 Hz to periods of hours. In some polycrystalline materials it is possible to see a decrease in conductivity associated with grain boundary effects at very low (about 1 Hz) frequencies. However, it may be seen from Figure 9 that dispersion is less than 2 hundredths of a log unit over 2 decades of frequency. It is difficult to envisage significant variation occurring in the next two decades to 1 Hz and certainly not an order of magnitude. We note that while magnetotelluric soundings of the mantle rely on relatively long-period observations, the work of Cox et al. [1986] was restricted to the frequency range of 1 to 24 Hz.

In spite of the excellent reproducibility we obtain in our measurements, we note here that on earlier runs, until the specimen equilibrated with the 10:1 mix at high temperatures, we observed a hysteresis amounting to 0.2–0.3 orders of magnitude in conductivity. The cause of this hysteresis is not known and is the subject of current investigation. However, the hysteresis disappears after equilibration with the 10:1 gas mix, and we have no reason to believe that this phenomenon compromises the interpretation of the data presented in this paper.

It is customary and reasonable to model mineral conductivity as the sum of several thermally activated processes:

$$\sum_i \sigma_i e^{-A_i/kT} \tag{5}$$

where the $A_i$ are activation energies, $\sigma_i$ are conductivities reflecting mobility and population of charge carriers of the various conduction mechanisms, $k$ is Boltzmann's constant and $T$ is absolute temperature. A single conduction mechanism in this model will generate a straight line on the $\log_{10}(\sigma) - 1/T$ plots normally used to present the data. Since one mechanism will usually dominate over a relatively wide temperature range, the data may be broken into regions where



Fig. 8. Dunite conductivity versus temperature for part of one run at 10:1 $CO_2$:CO mix. Heating [h] and cooling [c] cycles are indicated. The hysteresis at low temperature is probably due to the sample not reaching equilibrium after cooling from high temperatures; the larger defect population associated with the higher oxygen fugacity at high temperature has not yet been lost.

a linear relation holds and linear least squares fitting used to obtain $\log_{10}(\sigma_i)$ and $A_i$. Data in the transitions between conduction mechanisms must be neglected by this method, but it is relatively easy to perform an iterative nonlinear fit over several of the $i$ simultaneously, using, for example, the algorithm of Marquardt [1963]. Since the data in Figures 7 and 8 clearly represent two conduction mechanisms, and since we will shortly be making comparisons with single crystal data taken at higher temperature and exhibiting a third mechanism, we have used the Marquardt method to fit our data.

Table 2 gives the parameters fit to the heating cycles of both data sets presented in Figures 7 and 8, as well as the fits to previously published single crystal-data for comparison. The data and the fits are given in Figure 10. The errors presented in Table 2 are approximate; they are generated under the assumptions of local linearity and no covariance between the model parameters.

The data presented by Duba et al. [1974] have been carefully subsampled. We consider only those data collected under controlled oxygen fugacity, in which the authors used a gas mix equivalent to 30:1 $CO_2$:CO. Furthermore, it is known that the sample partially melted at the highest temperatures [Schock et al., 1989], and so we further restrict our choice to data during heating, up to a maximum of 1450°C. These data are plotted in Figure 10 using similar symbols to those in Duba et al.'s [1974] Figure 3. Fitting two conduction mechanisms to the RSP data yields the parameters given in Table 2. It comes as no surprise, since we are fitting the same model to the same data both using least squares, that $A_2$ = 1.53 eV agrees very well with the 1.51 eV given by Duba et al., but where we have obtained $A_3$ = 5.64 eV, Duba et al. obtained 2.74 and 7.89 eV by fitting two lines to what has been interpreted here as a single transition between $A_2$ and $A_3$ dominance. The data of T.J. Shankland and A. Duba (submitted manuscript, 1990) for the [010] direction of San Carlos olivine during the heating cycle are all within the transition between conduction mechanisms. The nonlinear fitting, however, produces activation energies similar to those for the RSP data. The ability to fit the data objectively within the transition between conduction mechanisms is the justification for, and advantage of, using the more complicated nonlinear modeling.

To determine the temperatures over which these conduction mechanisms are operative, we may set $\sigma_i e^{-A_i/kT} = \sigma_{i+1}e^{-A_{i+1}/kT}$ and solve for $T$. That is, we calculate the temperature at which both mechanisms in a transition have equal contribution to conductivity. We find from the JDC4 data that the transition from mechanism 1 to 2 occurs at 720°C. From the RSP[010] data the transition from mechanism 2 to 3 occurs at 1522°C and from SC[010] at 1515°C. Note that this temperature is higher than the 1390°C zero crossing of the thermoelectric coefficient observed by Schock et al. [1989], suggesting that the thermoelectric coefficient is not symmetrical about zero.

The agreement between the single-crystal data and the new polycrystalline data is astonishing. The activation energies for temperatures between 900° and 1200°C, where the data sets overlap (Figure 10), are virtually the same; $A_2$ = 2.45×10$^{-19}$ J for the RSP data and 2.56×10$^{-19}$ J for the JCD7 data. The agreement between the activation energies is substantial evidence that we are measuring olivine conduction in the dunite sample, unmodified by a grain boundary phase. (This contention is further supported by the similar oxygen fugacity dependence of the dunite and the single crystals.) The change in conduction mechanism below 700°C may represent a difficulty in controlling the oxygen fugacity, conduction in a grain boundary phase, or the growth of a low-temperature contaminant (other than carbon, which should not grow above 670°C in the worst case of 1:1 gas mix, and at much lower temperatures for the 10:1 and 50:1 mixes used to collect these lower temperature data). However, the reproducibility suggests that these too are measurements of olivine conductivity. There are no sources for comparison in the low-temperature region, as data for low-temperature conductivity have not been published for conductivity measured at controlled oxygen fugacity in single olivine crystals. Emphasis has always been placed on determining deep mantle conditions, and the difficulties in using controlled atmospheres and measuring high resistances have not been attacked previous to this work.

While the activation energies of the various samples are similar, the $\sigma_i$, reflected by the vertical position of the various curves in Figure 10, are not exactly the same. This is to be expected for a number of reasons:

First, the different oxygen fugacities used for the different

TABLE 2. Parametric Fits to Conductivity–Temperature Data

| Data Set | $i$ | $A_i$, J × 10$^{-19}$ | $A_i$, eV | $\log_{10}(\sigma_i$, S/m) | $N$ | % RMS |
|---|---|---|---|---|---|---|
| JCD4 | 1 | 0.21 ± 2.6 | (0.13 ± 1.60) | -5.7 ±9.6 | | |
| | 2 | 2.35 ± 5.9 | (1.47 ± 3.66) | 1.1 ±17. | | |
| | 3 | — | | — | 12 | 1.5 |
| JCD7 | 1 | — | | — | | |
| | 2 | 2.56 ± 0.02 | (1.60 ± 0.01) | 1.88 ±0.04 | | |
| | 3 | — | | — | 56 | 5.4 |
| RSP [010] | 1 | — | | — | | |
| | 2 | 2.45 ± 0.03 | (1.53 ± 0.02) | 1.74 ± 0.09 | | |
| | 3 | 9.0 ± 1.9 | (5.64 ± 1.17) | 13.3 ± 3.4 | 27 | 5.8 |
| SC [010] | 1 | — | | — | | |
| | 2 | 2.40 ± 0.03 | (1.50 ± 0.02) | 1.95 ± 0.07 | | |
| | 3 | 12.2 ± 1.0 | (7.61 ± 0.64) | 19.2 ± 1.8 | 66 | 1.9 |

The data used are the heating curve between 750° and 1200°C from Figure 8 (JCD7), the heating curve from the low temperature data in Figure 7 (JCD4), the subset of RSP data from Duba et al. [1974] described in the text and shown in Figure 10, and the [010] San Carlos olivine data (SC) of T.J. Shankland and A. Duba (submitted manuscript, 1990), also shown in Figure 10. $N$ is the number of data used in each fit and % RMS is the root mean square of the data residuals, expressed as a percentage of the linear conductivities.
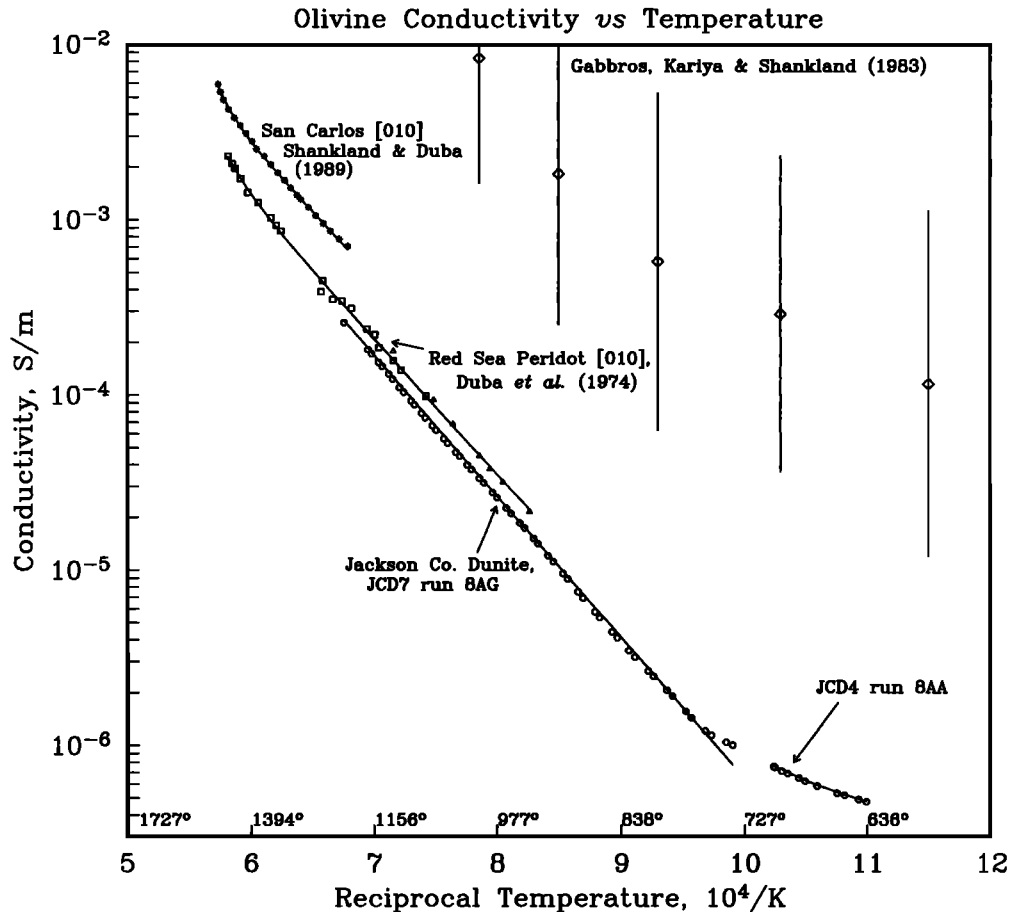
Fig. 10. Dunite conductivity versus temperature data [circles] compared with existing data from single crystals and rocks. Squares and triangles are measurements of a single crystal of Red Sea peridot in the [010] direction under controlled oxygen fugacity by *Duba et al.* [1974]. The asterisks are similar measurements on a crystal of San Carlos olivine by T.S. Shankland and A. Duba [submitted manuscript, 1989]. Heating data only are taken for all the olivines. The JCD4 data shown in Figure 7, which could be taken at lower temperatures because of the thinner sample size, lie below 700°C, while the higher temperature data are those shown in Figure 8. The diamonds and bars are means and standard deviations from a compilation of 37 measurements on gabbros by *Karyia and Shankland* [1983].

measurements will alter the conductivities. Measurements of RSP and JCD4 conductivity were made in an atmosphere corresponding to about $10^{-3}$ Pa $f_{O_2}$ at 1200°C, while the JCD7 data were taken in an atmosphere corresponding to $10^{-4.5}$ Pa. The San Carlos data were measured in an atmosphere of $10^{-4}$ Pa. Figure 5 shows the effect of variation in $f_{O_2}$ on olivines at 1200°C, but we are reluctant to use this to correct the $\sigma(1/T)$ curves. We have no information on the temperature dependence of the $f_{O_2}$ effects and no systematic data on conductivity as a function of $f_{O_2}$ for the particular RSP sample used by *Duba et al.* [1974].

Second, the conductivity of the dunite, which is composed of crystals having no preferred orientation, is the result of some sort of average of the conductivities of the three crystallographic axes. The single-crystal measurements, however, are along single axes, of which we have chosen [010] for our comparisons. (The [010] axis happens to be the most resistive.) The work of T.J. Shankland and A. Duba (submitted manuscript, 1990), who studied the effect of mixing data for the three axes to predict the conductivity of polycrystalline rock, indicates that conductivity in the [010] direction of the San Carlos olivine is 0.15 orders of magnitude lower than an average conductivity. Although we have used this result in Figure 6, we note that Figures 5 and 6 of *Shock*

*et al.* [1989] indicate that RSP anisotropy is more than twice that of the San Carlos olivine.

Iron content varies between the different samples. Although iron content is known to influence olivine conductivity [*Duba*, 1972], there is no systematic variation in conductivity as a function of iron for the various olivines under consideration. San Carlos olivine, $Fo_{91}$, has less iron than RSP, $Fo_{90}$, yet is more conductive. As we have seen, this matter is resolved not by looking at the conductivity–temperature data but by examining the conductivity–$f_{O_2}$ data. Inspection of the RSP oxygen fugacity data presented by *Schock et al.* [1989], taken on a different crystal than *Duba et al.* [1974], shows that at a similar oxygen fugacity this second specimen is about 0.20 orders of magnitude more conductive than the first, which also may be explained by the different iron content of the two specimens.

Finally, the concentration of charge carriers represented by our $\sigma_0$ term in equation (4) is clearly an intrinsic property of the olivine, and may vary from sample to sample even within the same olivine type.

## DISCUSSION

We see that after considering dependence on oxygen fugacity and random crystal orientations, the new conductivity

measurements on Jackson County dunite are in excellent agreement with previous single-crystal measurements on olivines. The similarity in conductivity, activation energy, and dependence of conductivity on oxygen fugacity all support the notion that conduction in the dunite is governed by olivine alone and that no correction of the single-crystal data need be made for grain boundary phases, grain boundary conduction, and minor phases such as oxides. Using a new parametric model for the conductivity dependence of olivine on oxygen fugacity, we see that the half order of magnitude variations between data sets can be explained by a combination of iron content and an intrinsic variation in an $f_{O_2}$ independent population of charge carriers. The real relationship between the conductivity behaviour of various olivines cannot be divined from the conductivity–temperature relationship but by the conductivity–$f_{O_2}$ dependence, as the activation energies of the various olivines are essentially the same.

On combining the various data sets discussed in this paper, the conductivity of an olivine dominated system can be described between $640°C$ and $1500°C$, a greater range than previously reported and spanning three conduction mechanisms. The conduction mechanism at the lowest temperatures has a very low activation energy, but without further experimentation, nothing more may be concluded. The mechanism that dominates between $720°$ and $1500°$ has an activation energy of $2.4$–$2.6 \times 10^{-19}$ J and is probably as described by Schock et al. [1989], whereby holes, generated by incorporating oxygen gas into the lattice, "hop" from one Fe site to another as they are trapped by $Fe^{++}$ to make $Fe^{+++}$. However, the independence of conductivity on $f_{O_2}$ below $10^{-5}$ Pa suggests that there is a population of conductors available for conduction which is independent of the oxygen environment.

Although data were not collected at temperatures relevant to the third conduction mechanism (greater than $1300°C$) in this study, the nonlinear fitting used here is able to determine an activation energy for this conduction mechanism from published conductivity data. The normal practice of fitting straight-line segments fails to utilize data at transition temperatures. However, at $1300°C$ temperatures are so compressed in $1/T$ space, and one is so close to the melting point of olivine at this $f_{O_2}$ that there is no room for a linear relationship to develop. The activation energy at these temperatures, obtained by taking a weighted average of the San Carlos and RSP fits, is $11.46 \pm 0.90 \times 10^{-19}$ J. Thanks to the work of Schock et al. [1989], we know that the charge carrier at these temperatures probably has a negative sign, and we have no cause to dispute their suggestion of magnesium vacancies as the charge carrier. Schock et al. [1989] suggest that opposing pressure coefficients for electronic and ionic conduction in a mixed hole and electron conduction model accounts for the low pressure coefficient observed in olivine by Duba et al. [1974]. However, a mixture of conduction mechanisms could only reduce the pressure effect in the transition region, yet the pressure dependence observed by Duba et al. [1974] is independent of temperature between $600°$ and $1400°C$. We have seen already that at $1200°C$ or below conduction is almost purely by means of one mechanism.

Duba et al. [1974] presented temperatures for the upper mantle by combining olivine conductivity to $1660°C$ with models for mantle conductivity derived from electromagnetic sounding. We now realize the dangers of melting and alteration at these high temperatures, so the recent measurements

of Schock et al. [1989] and our reinterpretation of the RSP data have been limited to about $1450°C$. Although we must therefore extrapolate the laboratory data to interpret mantle conductivity, the use of nonlinear fitting gives us the ability to estimate the activation energies at the highest temperatures. Extrapolation of our fit to the RSP data yields temperatures of $1575°$, $1720°$, and $1825°C$ at depths of 200, 300, and 400 km, using the conductivity model of Banks [1969]. (Banks' model is not significantly different from more recent interpretations using smooth modelling algorithms.) The more conductive San Carlos olivine yields cooler temperatures of $1515°$, $1625°$, and $1700°C$ at the same depths.

In view of the present work, there are no grounds for grain boundary conduction to be invoked in an olivine–rich mantle, and models based on single-crystal data are still the best available at temperatures high enough for silicate conduction to dominate. In any case, it becomes clear in hindsight that enhanced conduction is most unlikely to have the same activation energy as olivine, as is implied by a simple multiplicative factor applied to the single crystal conductivities. Indeed, it appears that, at a given temperature, variations in measurements between single crystal olivines and dunites alike are as dependent on oxygen fugacity as any other parameter. Until we have more confidence in our estimates of mantle oxygen fugacity (the reader is referred to the review by Ulmer et al. [1987]) there will be appreciable uncertainty in our predictions of mantle conductivity based on the laboratory data. For example, the difference between the wüstite–iron and quartz–fayalite–magnetite models of mantle oxidation state correspond to nearly an order of magnitude in conductivity for RSP at $1200°C$. Iron content also has an effect on conductivity; a 2% variation in Fe will produce a half order of magnitude variation in conductivity at high $f_{O_2}$. Besides changes in conductivity due to changes in oxygen fugacity and iron, there is half an order of magnitude variation in conductivity between various olivines at low oxygen fugacity. The reason for this variation is as yet unknown, but we speculate that it is a result of oxidation of the San Carlos olivine.

Examination of a polycrystalline sample has taken us one step closer to simulating the mantle environment in the laboratory. Our inability to apply pressure to the sample does mean, however, that thermal stresses will lessen the intimacy of grain to grain contact, so although the grain boundaries are present, they are limited in their ability to interact. It is therefore possible that in the mantle the dislocations formed by grain to grain boundaries could enhance conduction. It should be noted, however, that grains parting parallel to the measuring faces of the samples would lessen conduction, which was not observed. This suggests that grain parting was not a large effect, although we also note that several of the olivine crystals in the samples are large enough to span the two measurement faces.

The authors hope that the reader has gained an appreciation for how important it is that the experimental environment be properly controlled while making conductivity measurements. Almost any contamination or laboratory metamorphism of the sample, with the exception of iron loss, will result in an increased conductivity being observed. Few workers in the past have taken the basic precaution of controlling the oxygen in the atmosphere surrounding the sample. Inert atmospheres such as argon are inadequate as even minute levels of contamination with oxygen are likely to leave a substantial part of the experiment outside the stability field

of olivine. In a multiple phase system such as a rock it is even more difficult to ensure that all component minerals are within their stability fields, are in equilibrium with each other, and are in an environment that approximates Earth's interior. It is therefore not surprising that the compilation of conductivities for coarse-grained mafic rocks ("gabbros") made by *Kariya and Shankland* [1983] are at least one order of magnitude, and two on average, more conductive than the data presented here (Figure 10). Likely problems with these measurements are enhanced conduction due to water created by dehydration reactions and oxidation because of poor $f_{O_2}$ control during measurement.

*Cox et al.* [1986] performed a deep electrical sounding on the seafloor of the Pacific Ocean. In order to remove a strong correlation between model parameters, they used the RSP data of *Duba et al.* [1974] to provide a lower bound on mantle conductivity at depths where temperature would likely be the dominant control on conductivity. They also considered RSP×10 but used an upper bound on mantle conductivity based on rock measurements which was approximately RSP×100. Based on the present work, it may be seen that these upper bounds have little foundation in fact, and while there may indeed be factors which make upper mantle conductivity greater than that of its constituent olivine, these factors are as yet unknown and have not been produced in the laboratory. The model of Cox et al. which used an RSP model of mantle conductivity below 30 km constrained the topmost mantle between 5 and 30 km to be about $10^{-5}$ S/m. From the present work this is about 1.5 orders of magnitude greater than predicted by olivine conduction, lending support to Cox et al.'s proposal that traces of water are present in the oceanic upper mantle, or suggesting other conductivity enhancing phases dominate at depths where the temperature is below about 650°C.

## References

Astwood, P.M., J.R. Carpenter, and W.E. Sharp, A petrofabric study of the Dark Ridge and Balsam Gap dunites, Jackson County, North Carolina, *Southeast. Geol., 14*, 183-194, 1972.

Banks, R.J., Geomagnetic variations and the conductivity of the upper mantle, *Geophys. J.R. Astron. Soc , 17*, 457-487, 1969.

Bradley, R S., A.K. Jamil, and D.C. Munro, The electrical conductivity of olivine at high temperatures and pressures, *Geochim. Cosmochim Acta, 28*, 1669-1678, 1964.

Cox, C.S., S.C. Constable, A.D. Chave, and S.C. Webb, Controlled source electromagnetic sounding of the oceanic lithosphere, *Nature, 320*, 52-54, 1986.

Deines, P., R.H. Nafziger, G.C. Ulmer, and E. Woermann,Temperature -oxygen fugacity tables for selected gas mixtures in the system C-H-O at one atmosphere total pressure, bulletin, Earth and Miner. Sci. Exp. Stn., Pa. State Univ., University Park,1974.

Duba, A., The electrical conductivity of olivine, *J. Geophys. Res., 77*, 2483-2495, 1972.

Duba, A., Are laboratory electrical conductivity data relevant to the Earth?, *Acta Geophys. Montan. Acad. Sci. Hung., 11*, 485-495, 1976.

Duba, A., and I.A. Nicholls, The influence of the oxidation state on the electrical conductivity of olivine, *Earth Planet. Sci. Lett., 18*, 59-64, 1973.

Duba, A., J.N. Boland, and A.E. Ringwood, Electrical conductivity of pyroxene, *J. Geol., 81*, 727-735, 1973.

Duba, A., H.C. Heard, and R.N. Schock, Electrical conductivity of olivine at high pressure and under controlled oxygen fugacity, *J. Geophys. Res., 79*, 1667-1673, 1974.

Duba, A.G., R.N. Schock, E. Arnold, and T.J. Shankand, An apparatus to measure electrical conductivity to 1500 C at known oxygen fugacity, in *Ductile Transitions in Rocks, The Heard Volume, Geophys. Mono. Ser.*, edited by A. Duba, W. Durham, J. Handin and H. Wang, in press, AGU, Washington, D.C., 1990.

Huebner, J.S., Buffering techniques for hydrostatic systems at elevated pressures, in *Research Techniques for High Pressure and High Temperature*, edited by G.C. Ulmer, pp. 123-177, Springer-Verlag, New York, 1971.

Jones, A.G., On the electrical crust-mantle structure in Fennoscandia: no Moho and the asthenosphere revealed?, *Geophys. J.R. Astron. Soc., 68*, 371-388, 1982.

Karato, S., M.S. Paterson, and J.D. FitzGerald, Rheology of synthetic olivine aggregates: Influence of grain size and water, *J. Geophys. Res., 91*, 8151-8176, 1986.

Kariya, K.A., and T.J. Shankland, Electrical conductivity of dry lower crustal rocks, *Geophysics, 48*, 52-61, 1983.

Lipin, B.R., Chromite from the Blue Ridge Province of North Carolina, *Am. J. Sci., 284*, 507-529, 1984.

Marquardt, D.W., An algorithm for least-squares estimation of nonlinear parameters, *J. Soc. Ind. Appl. Math., 11[2]*, 431-441, 1963.

Misra, K.C. and F.B. Keller, Ultramafic bodies in the southern Appalachians: A review, *Am. J. Sci., 278*, 389-418, 1978.

Schock, R.N., and A.G. Duba, Point defects and the mechanisms of electrical conduction in olivine, in *Point Defects in Minerals, Geophys. Mono. Ser. vol. 31*, edited by R. N. Schock, pp. 88-96, AGU, Washington, D.C., 1985.

Schock, R.N., A.G. Duba, H.C. Heard, and H.D. Stromberg, The electrical conductivity of polycrystalline olivine and pyroxene under pressure, in *High Pressure Research: Applications in Geophysics*, edited by M. Manghani and S. Akimoto, pp. 39-51, Academic, San Diego, Calif., 1977.

Schock, R.N., A. Duba, and T.J. Shankland, Electrical conduction in olivine, *J. Geophys. Res., 94*, 5829-5839, 1989.

Shankland, T.J., Transport properties of olivine, in *Application of Modern Physics to the Earth and Planetary Interiors*, edited by S.K. Runcorn, pp. 175-190, Wiley-Interscience, New York, 1969.

Shankland, T.J., Electrical conduction in mantle materials, in *Evolution of the Earth, Geodyn Ser., vol. 5*, edited by R.J. O'Connell and W.S. Fyfe, pp. 256-263, AGU, Washington D.C., 1981.

Shankland, T.J., and H.S. Waff, Partial melting and electrical conductivity anomalies in the upper mantle, *J Geophys. Res., 82*, 5409-5417, 1977.

Ulmer, G.C., D.E. Grandstaff, D. Weiss, M.A. Moats, T.J. Buntin, D.P. Gold, C.H. Hatton, A. Kadik, R.A. Koseluk, and M. Rosenhauer, The mantle redox state: An unfinished story?, *Mantle Metasomatism and Alkaline Magmatism*, edited by E.M. Morris and J.D. Pasteris, *Geol. Soc. Am. Spec Pap., 215*, 5-23, 1987.

S. Constable, Scripps Institution of Oceanography, Mail Code A025, La Jolla, CA 92093.

A. Duba, Lawrence Livermore National Laboratory, Livermore, CA 94550.